

## ORIGINAL ARTICLE

# Overexpression of ARHGAP30 suppresses growth of cervical cancer cells by downregulating ribosome biogenesis

Aijia Wu<sup>1</sup> | Lan Lin<sup>1</sup>  | Xiao Li<sup>1</sup> | Qinyang Xu<sup>1</sup> | Wei Xu<sup>1</sup> | Xiaolu Zhu<sup>1</sup> | Yincheng Teng<sup>1</sup> | Xiao-Mei Yang<sup>2</sup> | Zhihong Ai<sup>1</sup> 

<sup>1</sup>Department of Obstetrics and Gynecology, Shanghai Jiao Tong University Affiliated Sixth People's Hospital, Shanghai, China

<sup>2</sup>State Key Laboratory of Oncogenes and Related Genes, Shanghai Cancer Institute, Ren Ji Hospital, School of Medicine, Shanghai Jiao Tong University, Shanghai, China

**Correspondence**

Xiao-Mei Yang, State Key Laboratory of Oncogenes and Related Genes, Shanghai Cancer Institute, Ren Ji Hospital, School of Medicine, Shanghai Jiao Tong University, 800 Dongchuan Road, Shanghai 200240, China.  
Email: xmyang@shsci.org

Zhihong Ai, Department of Obstetrics and Gynecology, Shanghai Jiao Tong University Affiliated Sixth People's Hospital, No.600 Yishan Road, Shanghai 200233, China.  
Email: ai\_zhihong@126.com

**Funding information**

Natural Science Foundation of Shanghai (grant/award number: 17ZR1421400)

**Abstract**

We aimed to identify whether Rho GTPase activating proteins (RhoGAPs) were downregulated in cervical cancers and might be targeted to reduce the growth of cervical cancer using the GEO database and immunohistochemical analysis to identified changes in transcription and protein levels. We analyzed their proliferation, clone formation ability, and their growth as subcutaneous tumors in mice. To detect ARHGAP30 localization in cells, immunofluorescence assays were conducted. Mass spectrometry combined with immunoprecipitation experiments were used to identify binding proteins. Protein interactions were validated with co-immunoprecipitation assays. Western-blot and q-PCR were applied to analyze candidate binding proteins that were associated with ribosome biogenesis. Puromycin incorporation assay was used to detect the global protein synthesis rate. We identified that ARHGAP30 was the only downregulated RhoGAP and was related to the survival of cervical cancer patients. Overexpression of ARHGAP30 in cervical cancer cells inhibited cell proliferation and migration. ARHGAP30 immunoprecipitated proteins were enriched in the ribosome biogenesis process. ARHGAP30 was located in the nucleus and interacted with nucleolin (NCL). Overexpression of ARHGAP30 inhibited rRNA synthesis and global protein synthesis. ARHGAP30 overexpression induced the ubiquitination of NCL and decreased its protein level in HeLa cells. The function of ARHGAP30 on cervical cancer cell ribosome biogenesis and proliferation was independent of its RhoGAP activity as assessed with a RhoGAP-deficient plasmid of ARHGAP30<sup>R55A</sup>. Overall, the findings revealed that ARHGAP30 was frequently downregulated and associated with shorter survival of cervical cancer patients. ARHGAP30 may suppress growth of cervical cancer by reducing ribosome biogenesis and protein synthesis through promoting ubiquitination of NCL.

**KEYWORDS**

ARHGAP30, cervical cancer, nucleolin, ribosome biogenesis, ubiquitination

**Abbreviations:** ACTB,  $\beta$ -actin; IRB, institutional review boards; NCL, nucleolin; OS, overall survival; RhoGAPs, Rho GTPase activating proteins.

Aijia Wu, Lan Lin and Xiao Li contributed equally to this manuscript.

This is an open access article under the terms of the Creative Commons Attribution-NonCommercial-NoDerivs License, which permits use and distribution in any medium, provided the original work is properly cited, the use is non-commercial and no modifications or adaptations are made.

© 2021 The Authors. *Cancer Science* published by John Wiley & Sons Australia, Ltd on behalf of Japanese Cancer Association.

## 1 | INTRODUCTION

Cervical cancer is the most common gynecological tumor worldwide. The latest data from the International Agency for Research on Cancer reported 570 000 cervical cancer cases diagnosed and 311 000 deaths in 2018.<sup>1</sup> Some patients have bad prognosis and low quality of life when diagnosed as advanced-stage or high-grade histology. In advanced-stage patients, external-beam radiation therapy, chemotherapy, and brachytherapy were recommended. Cisplatin was the most active single agent, but its reported response rate only reached 20%-30%. Data from 411 studies found that overall survival (OS) with cisplatin alone in metastatic patients was 6.5-9 months.<sup>2</sup> It is therefore meaningful to study the pathogenic mechanisms of cervical cancer and seek new prognostic markers and targets for cervical treatment.

In cervical cancers, the activities of Rac1 and RhoA were frequently elevated and upregulated and were related to patients' worse prognosis.<sup>3,4</sup> RhoA and Rac1 are important members of small GTPase. Rho GTPase activating proteins (RhoGAPs) belong to the RAS superfamily and control critical biological processes in cancer tumorigenesis and tumor metastasis. RhoGAPs elevated the intrinsic activity of RhoGTPase and accelerated hydrolysis of GTP to GDP. Recent studies found that RhoGAPs were frequently downregulated in some human cancers.

In this study, using the GEO database, we compared the gene expression profiles in cervical cancer microarray datasets and found ARHGAP30 was significantly downregulated in cervical cancers. ARHGAP30 is a RhoGAP specific for the activity of Rac1 and RhoA. A previous study suggested ARHGAP30 was a Wrch-1-interacting protein that regulated actin dynamics and cell adhesion.<sup>5</sup> Wang et al<sup>6</sup> found that ARHGAP30 promoted p53 acetylation and functional activation in colorectal cancer. ARHGAP30 was also found to inhibit the Wnt/ $\beta$ -catenin pathway in lung cancer and pancreatic cancer to suppress their progression.<sup>7,8</sup> To date, the function and underlying molecular mechanism of ARHGAP30 in cervical cancer progression remains unclear.

Ribosomes are essential for protein production in all living cells. Ribosome synthesis increases in cancer cells to cope with an increase in protein synthesis and sustained unrestricted growth.<sup>9</sup> Ribosome biogenesis occurs in the nucleolus during the interphase and nucleolin (NCL) is one of the most abundant nucleolar proteins known to play a critical role in the process of ribosome biogenesis.<sup>10</sup> NCL interacts transiently with rRNA and pre-ribosomal particles. Previous studies suggested that NCL functions as multiprotein complexes during ribosome biogenesis and maturation.<sup>10</sup> In addition, NCL might also be involved in several pre-mRNA processing pathways such as pre-mRNA splicing, transport, or stability.<sup>11</sup> NCL works as an activator of human papillomavirus type 18 oncogene transcription, directly linked to cervical carcinogenesis.<sup>12</sup> Immunostaining tests showed that the expression level of NCL was significantly higher in invasive cervical squamous cell carcinoma than in normal cervical epithelia tissues.<sup>13</sup>

Here we found that ARHGAP30 overexpression suppressed the proliferation of cervical cancer cells in vitro and in vivo, inhibited cell migration, and promoted cell apoptosis. ARHGAP30 was accumulated in the nucleolus and colocalized with NCL. Mass spectrometry and co-immunoprecipitation experiments showed that ARHGAP30 interacted with NCL. Furthermore, we found that ARHGAP30 promoted the ubiquitination of NCL and facilitated NCL degradation, accompanied by decreased global protein synthesis. Our study illustrated a tumor-suppressing role of ARHGAP30 in cervical carcinogenesis that acted through counteracting nucleolar NCL to suppress ribosome biogenesis.

## 2 | MATERIAL AND METHODS

### 2.1 | Patients and cervical cancer biopsy specimens

Twenty patients with pathologically confirmed cervical cancer were enrolled and underwent surgery at Shanghai Sixth People's Hospital affiliated to the Shanghai JiaoTong University School of Medicine between January 2016 and December 2018. IRB approval was obtained for using these samples. Both cervical cancer and paired normal tissues (taken at least 5 cm away from the tumor and confirmed to be normal by histological examinations) were analyzed for ARHGAP30 protein expression by immunohistochemical staining.

### 2.2 | Cell culture

The human cervical cancer cell lines Hela and C33A were all preserved in Shanghai Sixth People's Hospital, School of Medicine, Shanghai Jiao Tong University. All cell lines were cultured in DMEM medium (Hyclone) supplemented with 10% fetal bovine serum (BI).

### 2.3 | Overexpression of ARHGAP30

Plasmid overexpressing ARHGAP30-Flag was constructed by linking the full length human ARHGAP30 cDNA with the pLenti-CMV-MCS-3FLAG-PGK-Puro vector. Plasmid overexpressing ARHGAP30-EGFP-Flag to monitor the localization of ARHGAP30 was constructed by linking full-length human ARHGAP30 cDNA with pLenti-CMV-EGFP-3FLAG vector (OBiO Technology). RhoGAP-deficient ARHGAP30 plasmid was constructed by linking ARHGAP30<sup>R55A</sup> mutant cDNA with pLenti-CMV-EGFP-3FLAG vector (OBiO Technology). Lentivirus was produced by co-transfecting lentiviral plasmid and package plasmids into 293T cells. Cells were infected by lentivirus for 48 h and then selected by 2  $\mu$ g/mL puromycin for 48 h. Cells overexpressing ARHGAP30-Flag were used for CCK8, colony formation, cell apoptosis assays, Transwell, affinity capture, and mass spectrometry. Cells overexpressing ARHGAP30-EGFP-Flag were used in the analysis of subcellular localization of

ARHGAP30 by immunofluorescence and also in the puromycin incorporation assay.

## 2.4 | Cell proliferation, colony formation, and cell apoptosis assays

The cell proliferation was determined using CCK-8 (Dojindo Laboratories) assay. Cell viability was monitored by measuring absorbance at 450 nm using a Power Wave XS microplate reader (Infinite M100 pro, TECAN). The experiment was performed in quintuplicate and repeated twice. Colony formation was performed to evaluate anchorage-independent growth. After 21 days, colonies were fixed with 4% PFA, stained with crystal violet and counted by microscopy. For cell apoptosis, cells were serum-free starved for 24 h and then collected and stained with 50 mg/mL propidium iodide and Annexin V-fluorescein isothiocyanate (Dojindo Laboratories) following the manufacturer's instructions. The percentage of Annexin V (+) and propidium iodide (+) cells was analyzed by flow cytometry.

## 2.5 | Transwell assay

The migration assays were performed using a Transwell chamber (Millipore). Cells were seeded into the upper chamber with serum-free medium ( $5-8 \times 10^4$  cells), and the bottom of the chamber contained the DMEM medium with 10% FBS. After 24 h, cells migrating through the pore were fixed and stained with crystal violet, and images were acquired at the same magnification. Results were based on four independent experiments (Student's *t* test).

## 2.6 | Immunohistochemistry

Immunohistochemistry (IHC) was performed as previously reported.<sup>14</sup> Immunohistochemical staining results were scored without prior knowledge of details. Protein staining was scored as two groups: positive and negative (no appreciable staining in tumor cells). The final result was satisfied with chi-square test.

## 2.7 | Animal studies

Animal experiments were approved by the Laboratory Animal Center of Shanghai Jiao Tong University. All animals received humane care according to the criteria outlined in the Guide for the Care and Use of Laboratory Animals prepared by the National Academy of Sciences and published by the National Institutes of Health. Female BALB/c nude mice (6 weeks old, 15–18 g) received single subcutaneous flank injection of  $8 \times 10^6$  Lenti-vector or Lenti-ARHGAP30 HELA cells ( $n = 5$  per group) in 150  $\mu$ L PBS. Five weeks

after injection, the mice were sacrificed and the tumors were harvested. The tumor volume was evaluated using the following formula:  $V = (\text{length}) \times (\text{width}) \times (1/2 \text{ width})$ .

## 2.8 | q-PCR

Cervical cancer cells were harvested and lysed in TRIzol (Invitrogen). Reverse transcription was performed as described.<sup>14</sup> ARHGAP30 primers: 5'-GGAGGAGTATGGAGTGGTGGATGG-3' (forward), 5'-AGGTCTGGCTCCGCTCTGAC-3' (reverse).

## 2.9 | Western blot assay

Western blot analysis was performed as described.<sup>14</sup> The antibodies used were anti-ARHGAP30 Ab (Abcam), DYKDDDDK Tag Polyclonal Antibody (Proteintech Group), Flag-Tag Monoclonal Antibody (Abways Technology), NCL Polyclonal Antibody (Proteintech Group), anti- $\beta$ -actin Ab (Abways Technology), anti-Ubiquitin antibody (P4D1; Santa Cruz Biotechnology), Lamin B1 Antibody (Abways Technology), and alpha Tubulin Antibody (Abways Technology).

## 2.10 | Affinity capture and mass spectrometry

Protein A/G magnetic beads (Bimake) were incubated with 2  $\mu$ g of anti-Flag antibody or equivalent IgG for 15 min. HeLa cells overexpressing ARHGAP30-Flag were lysed with cell lysis Buffer (Sangon Biotech) and centrifuged. Supernatants were then incubated with anti-Flag antibody bound magnetic beads (Bimake) for 45 min. Bound proteins were eluted from the magnetic beads and were subjected to SDS-PAGE. Gels were stained with Coomassie Blue, and the electrophoresis lanes were dissected and subjected to mass spectrometry analysis (Q Exactive HF-X Hybrid Quadrupole-Orbitrap MS, Thermo Scientific).

## 2.11 | Immunofluorescence

Cells transfected with vector and ARHGAP30-EGFP were inoculated in an eight-well u-Chamber (Ibidi). Cells were then fixed with 4% paraformaldehyde at room temperature for 15 min and permeabilized with 0.1% Triton X-100 for 5 min. The cells were blocked with 1% bovine serum albumin at room temperature for 1 h, then incubated with primary antibodies against NCL Polyclonal Antibody (Proteintech Group), NPM Antibody (Abcam) and with species-matched secondary antibodies conjugated with Alexa Fluor-594. The nucleus was stained with DAPI (D9542, Sigma-Aldrich) for 8 min at room temperature and the immunofluorescence images were acquired with confocal microscopy (Carl Zeiss).

## 2.12 | Puromycin incorporation assay

Puromycin is an aminonucleoside antibiotic, derived from the *Streptomyces alboniger* bacterium, that causes premature chain termination during translation taking place in the ribosome. Part of the molecule resembles the 3' end of the aminoacylated tRNA, making it useful for protein translation analysis.<sup>15,16</sup> Cultured vector cells and ARHGAP30 overexpression cells were treated with 10  $\mu\text{mol/L}$  for 20 min during the growth phase (40%-50% confluence). Newly synthesized proteins were labelled by puromycin. After cell counting, cells were lysed with RIPA lysis with 1 mmol/L PMSF and Protease inhibitor cocktail. Total proteins were separated by 10% SDS-PAGE gel and detected by an antipuromycin monoclonal antibody (Kerafast).

## 2.13 | Ubiquitination assay

pCMV-V5-Ub plasmid (OBiO Technology) was transfected to indicated cells to induce Ub overexpression. Cells were treated with or without 5  $\mu\text{mol/L}$  MG132 for 12 h before they were collected and lysed. Immunoprecipitation of NCL protein was performed using anti-NCL antibody bound protein A/G magnetic beads. Bound proteins were subjected to SDS-PAGE electrophoresis and blotted with the anti-ubiquitin antibody (Santa Cruz Biotechnology).

# 3 | RESULTS

## 3.1 | ARHGAP30 was downregulated in cervical cancer tissues and related to poor prognosis

To unveil the differentially expressed RhoGAPs genes in cervical cancers, we compared gene expression profiles across two analyses containing microarray datasets via the GEO database (GSE6791 and GSE7410). Nineteen RhoGAPs genes in GSE6791 and 13 genes in GSE7410 were downregulated compared to their normal counterparts, with nine overlapped genes (Figure 1A,B). Low ARHGAP30 mRNA expression was correlated with poor overall survival (OS:HR:0.44,  $P = .014$ ) analyzed in the Kaplan-Meier plotter database while other RhoGAPs were not (Figures 1D and S1). Low ARHGAP30 mRNA expression was also correlated with poor progression-free survival (PFS: HR: 0.29,  $P = .045$ ). We analyzed ARHGAP30 expression in cervical datasets of GSE7410 containing 40 tumor and five normal samples, and GSE6791 containing 20 tumors and eight normal tissues. Both datasets showed that the mRNA ARHGAP30 level was significantly lower in cervical tumor tissues ( $P = .03$  for GSE7410 and  $P < .01$  for GSE6791; Figure 1C). To confirm the decreased expression of ARHGAP30 in cervical cancers, we performed IHC staining using a cervical cancer microarray containing 10 cancers and 10 normal tissues, and the results showed that ARHGAP30 was significantly downregulated in cervical cancers ( $P = .006$ ; Figure 1E).

## 3.2 | ARHGAP30 suppressed cervical cancer growth and migration, and promoted apoptosis

To investigate the biological role of ARHGAP30 in cervical cancer, Hela and C33A cells were infected with lenti-ARHGAP30 or lenti-vector virus. Lentivirus-mediated overexpression of ARHGAP30 was validated by q-PCR and western blot (Figure 2A,B). Cell proliferation and the colony formation ability of cervical cancer cells were suppressed by overexpression of ARHGAP30 (Figure 2C,D). In the nude mouse xenograft model, tumor weights and tumor volumes in mice with injection of HELA-Vector cells were larger than those in HELA-OV group (Figure 2E). Transwell assays showed that overexpression of ARHGAP30 led to fewer cells migrating through the 8  $\mu\text{m}$  pore of the chamber, compared to the control group (Figure 2F). Furthermore, we performed a serum-free induced cell apoptosis assay. The results showed that the apoptotic rate was increased by overexpression of ARHGAP30 (Figure 2G). These results demonstrate a suppressing role of ARHGAP30 in cervical cancer progression.

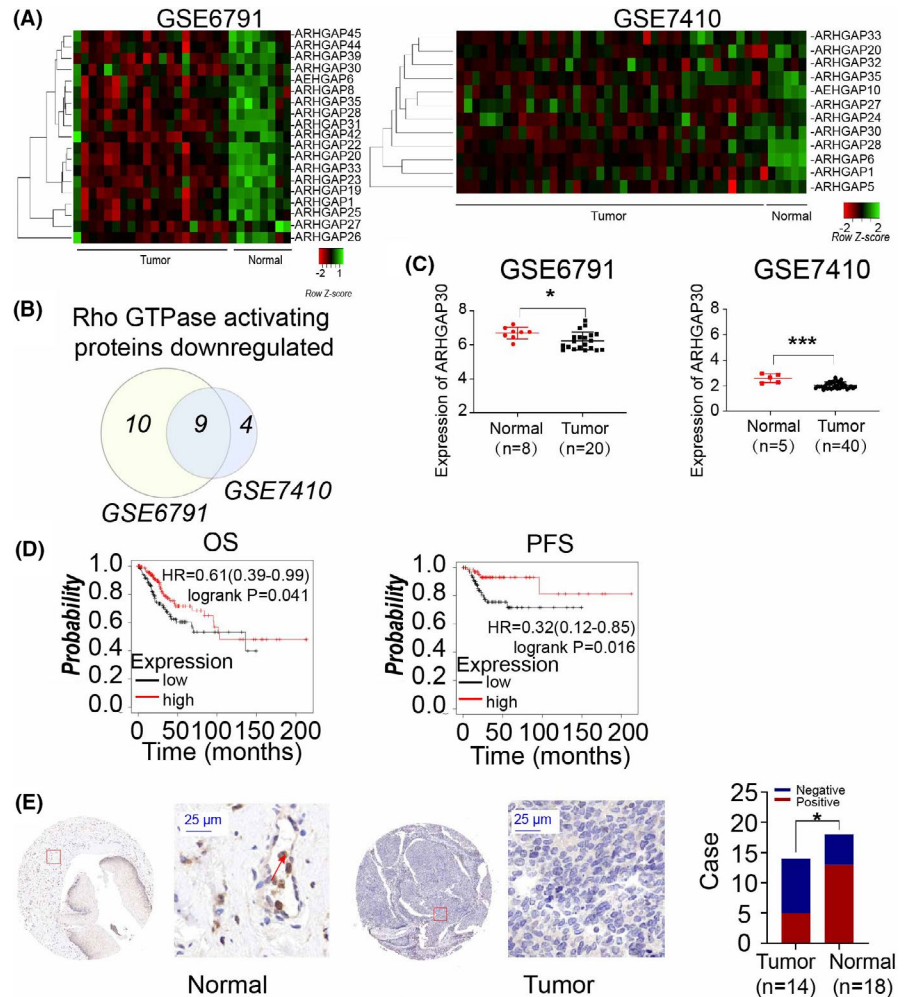
## 3.3 | ARHGAP30 was located in the nucleolus and related to ribosome biogenesis

Next, by immunofluorescence staining, we found that ARHGAP30-EGFP was located in both nucleus and cytoplasm of HELA and C33A cells, and in the nucleolus ARHGAP30 was co-located with nucleolar NPM (Figure 3A). The nucleolus is an important dynamic organelle responsible for the ribosome RNA biogenesis and ribosomal subunits assembly,<sup>17</sup> but the role of ARHGAP30 in nucleolus formation and ribosome biogenesis has not been discovered. Interestingly, when we performed immunoprecipitation of ARHGAP30-3Xflag and subsequent LC-MS analysis of co-precipitated proteins in ARHGAP30-3Xflag overexpressing Hela cells, we identified 166 high score proteins that formed complexes with ARHGAP30 (Table S1). These proteins were mostly enriched in ribosome biogenesis-related processes and were largely associated with nucleus and nucleolus apparatus by gene ontology analysis and KEGG pathway analysis (Figure 3B,C). These results imply that ARHGAP30 may have a regulatory role of ribosome biogenesis in the nucleolus of cervical cancer cells.

## 3.4 | ARHGAP30 suppressed cervical cancer growth by reducing global protein synthesis

By semiquantitative q-PCR analysis, we found that pre-rRNA, 5.8s rRNA, and 28s rRNA were significantly reduced by overexpression of ARHGAP30, while 18s rRNA was not changed (Figure 3D). This implies that ARHGAP30 is a negative regulator for rRNA transcription and ribosome biogenesis, thus ARHGAP30 might have a suppressing role in nascent protein synthesis in cervical cancer cells. As puromycin resembled the 3' end of the aminoacylated tRNA, it can be conjugated to the nascent peptide chains and detected by

**FIGURE 1** ARHGAP30 was downregulated in cervical cancers and correlated with patient prognosis. A, Heatmap of Rho GTPase activating proteins downregulated in GEO database GSE6791 and GSE7410. We selected adj *P* value <.05 as cut off. B, Venn plot showing the overlap Rho GTPase activating proteins downregulated in both GSE6791 and GSE7410. C, ARHGAP30 mRNA level in cervical cancer tissues vs normal cervix tissue. D, Kaplan-Meier plot of the correlation between ARHGAP30 expression and patient survival, using TCGA databases. E, Representative immunohistochemical images of ARHGAP30 expression and its regional magnification in tissues (left). Red arrows indicated dominant nucleolus localization of ARHGAP30 in normal cervix cells. The constituent ratio of ARHGAP30 expression assessed by blinded IHC analyses in normal tissues (*n* = 10) and cervical cancer tissues (*n* = 10; right). Scale bar indicates 25  $\mu$ m. \**P* < .05; \*\**P* < .01; \*\*\**P* < .001



immunoblot analysis with an antibody against puromycin (3RH11). We treated ARHGAP30 overexpressing and control cervical cancer cells with puromycin (10  $\mu$ g/mL) for 20 min and extracted cell lysates for western blot analysis with an anti-puromycin antibody. The results showed that overexpression of ARHGAP30 led to reduced rates of global protein synthesis in both HeLa and C33A cells (Figure 3E). In cancer cells, the rates of protein biosynthesis were tightly correlated with the rate of cell growth and proliferation.<sup>18</sup> These results therefore suggest that ARHGAP30 suppresses cervical cancer growth through downregulating ribosome biogenesis and global protein synthesis.

### 3.5 | ARHGAP30 interacted with NCL and regulated its nucleolus expression

Previous study revealed the interaction of ARHGAP30 and acetyltransferase p300, and the involvement of ARHGAP30 in p53 acetylation and activation.<sup>6</sup> Ko<sup>19</sup> revealed acetylation of NCL by p300 and ubiquitin-dependent degradation of deacetylated NCL. To address possible interaction of ARHGAP30 with p300 in cervical cancer cells, we performed co-immunoprecipitation experiments and found

that p300 was not co-immunoprecipitated with ARHGAP30 in HeLa cells and C33A cells (Figure S2A).

P300 was neither a prey of ARHGAP30 by analyzing ARHGAP30-3Xflag bound proteins in the mass spectrometry dataset. Interestingly, we found NCL was a noticeable prey of ARHGAP30. NCL is one of the most abundant nucleolar proteins and is known to interact transiently with rRNA and preribosomal particles. NCL participated in modulating rDNA transcription, RNA metabolism, and ribosome assembly and was critical in ribosome biogenesis and maturation.<sup>10,20</sup> Co-immunoprecipitation experiments using an anti-Flag antibody or an anti-NCL antibody confirmed the interaction between NCL and ARHGAP30 (Figure 4A). By semiquantitative analysis of the mRNA and protein level of NCL, we found overexpression of ARHGAP30 clearly reduced the NCL protein level without affecting its mRNA level (Figure 4B). Detection of NCL in nuclear/cytosol fractionations showed that nuclear NCL was decreased by overexpression of ARHGAP30 (Figure 4C). Immunofluorescence of NCL further confirmed that ARHGAP30-EGFP overexpressing in cervical cancer cells reduced NCL expression in the nucleolus (Figure 4D). Global proteomics and interactomic assay showed NCL interacted with polymerase (RNA) I,<sup>11</sup> which was responsible for transcription of pre-rRNA, 28S, and 5.8S rRNA. These results indicate that

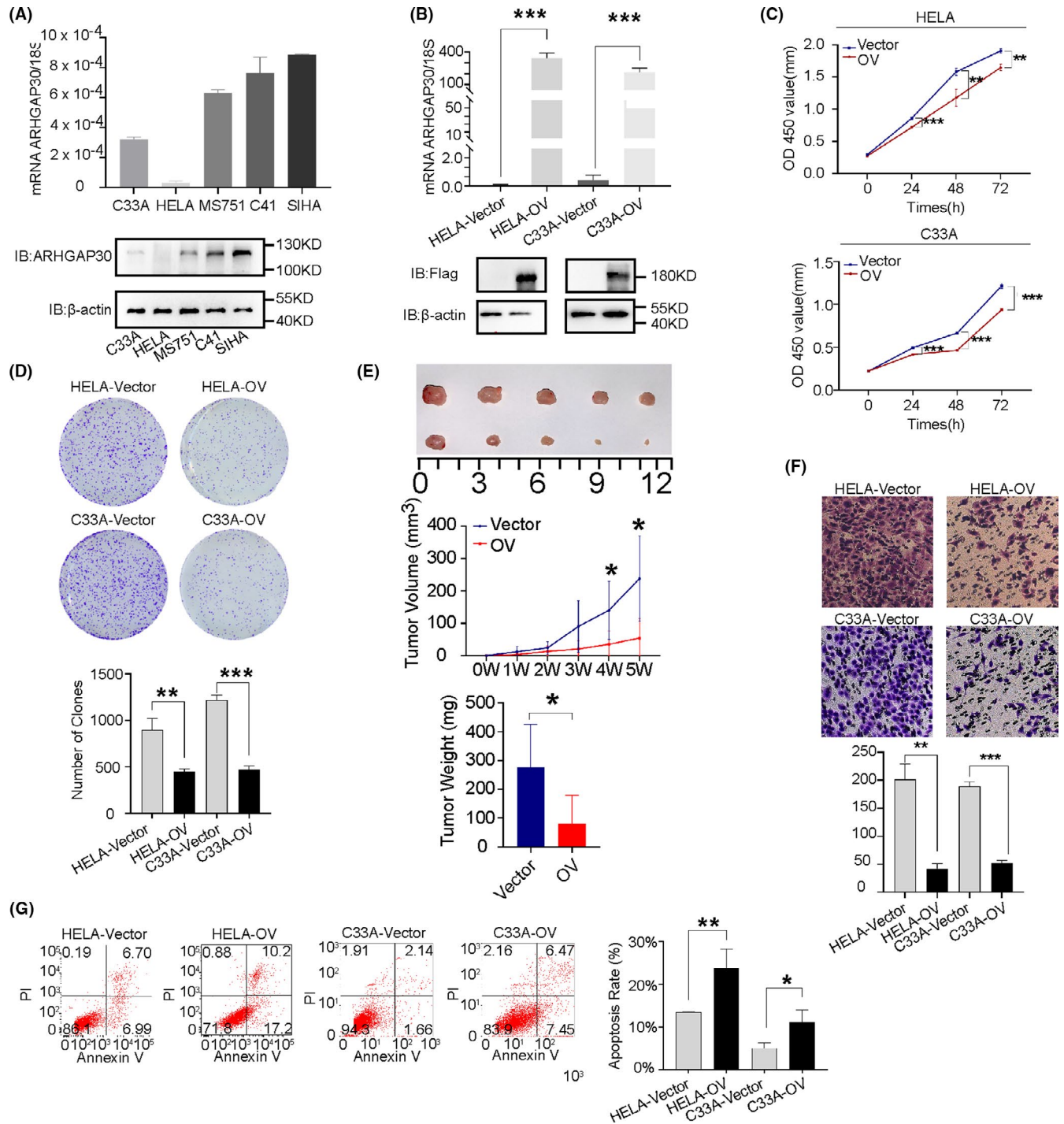


**FIGURE 2** ARHGAP30 inhibited cervical cancer growth in vitro and in vivo. A, Upper panel: ARHGAP30 mRNA level in various cervical cancer cell lines. Lower panel: ARHGAP30 protein level in various cervical cancer cell lines with ACTB detected as the internal control. B, Validation of ARHGAP30 overexpression in cervical cancer cell lines using rt-PCR and Western blot analysis. Flag antibody was detected for overexpression of ARHGAP30. C, Analysis of cervical cancer cell proliferation in vitro. Results are shown as the means  $\pm$  standard deviation of the OD 450 value. D, Anchorage-independent colony formation analysis. Statistical analysis is shown in the lower panel. E, Subcutaneous tumor growth in mice inoculated with HELA-OV or HELA-Vector cells. Each group of mice was randomly divided into two groups ( $n = 5$  per group). Upper, Photos of tumors; middle, growth curve of tumors; lower, statistical analysis of tumor weight growth over 5 weeks. Data shown are the mean  $\pm$  standard deviation. P values were calculated by t test. F, Representative images for Transwell migration assays and statistical analysis (lower panel). G, Apoptosis analysis of cells with or without ARHGAP30 overexpression. PI, propidium iodide. Statistical analysis is shown in the right panel. \* $P < .05$ ; \*\* $P < .01$ ; \*\*\* $P < .001$

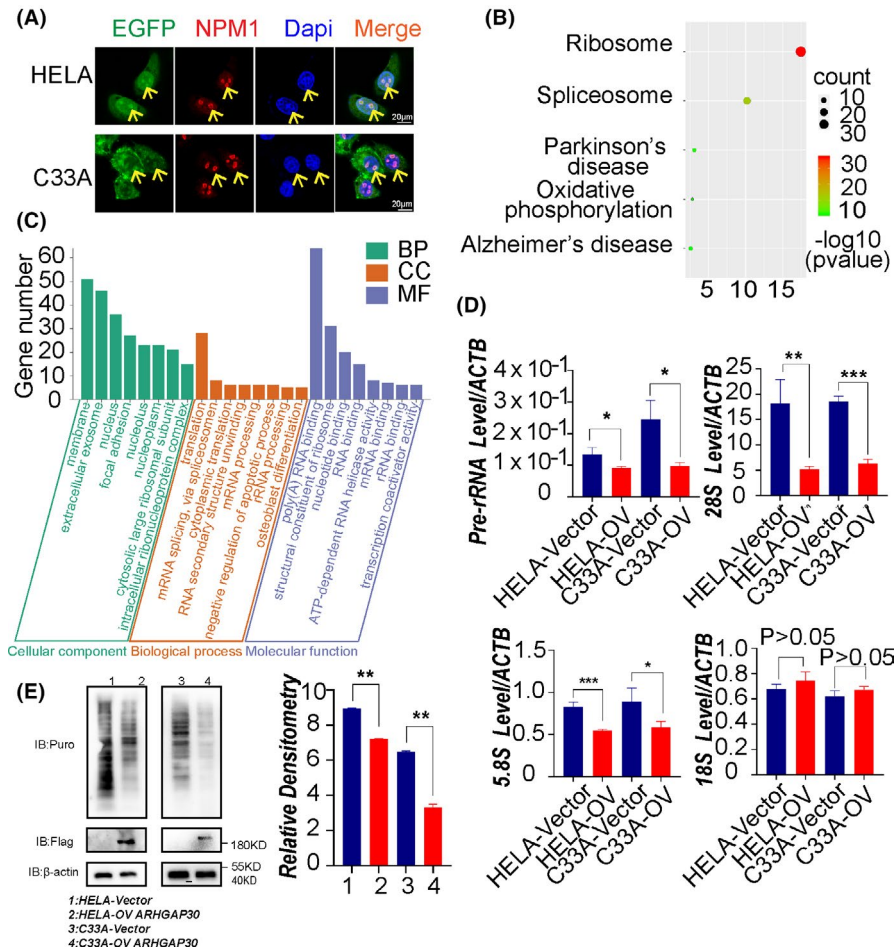


**FIGURE 3** ARHGAP30 was located in nucleolus and was related with ribosome biogenesis. A, Immunofluorescence staining of NPM1 in HELA ARHGAP30-EGFP and C33A ARHGAP30-EGFP cells. Nucleolus was indicated with yellow arrows. HELA ARHGAP30-EGFP and C33A ARHGAP30-EGFP were cervical cancer cells overexpressed with ARHGAP30-EGFP fusion protein. Scale bar: 20  $\mu$ m. B, KEGG pathway enrichment of ARHGAP30 captured proteins in HELA-OV cells. KEGG, Kyoto Encyclopedia of Genes and Genomes. C, GO analysis of ARHGAP30 captured proteins in HELA-OV cells. The y axis represents gene numbers, the x axis represents BP, MF, and CC terms. The top eight gene ontology entries are listed. BP, biological process; MF, molecular function; CC, cellular component. D, Analysis of pre-rRNA, 28S, 5.8S, and 18S rRNA level in HELA-OV, C33A-OV, and their paired control cancer cells, normalized to  $\beta$ -actin (ACTB). E, Western blot of puromycin-labeled nascent proteins. Puromycin (10  $\mu$ mol/L) was added to the medium of HELA and C33A cells 20 min before harvest. Anti-Flag antibody was used to detect the exogenous expression of ARHGAP30-Flag. ACTB was detected as an internal control. Relative quantification of the density of western blot bands is shown in the right panel

ARHGAP30 suppresses rRNA synthesis and proliferation of cervical cancer cells through counteracting NCL.

### 3.6 | ARHGAP30 promoted NCL ubiquitylation and degradation

We next examined the stability of NCL by adding cycloheximide (CHX) to inhibit protein synthesis. On treatment with CHX (25  $\mu$ g/mL CHX) for 8, 12, and 24 h, the protein level of NCL decreased dramatically in ARHGAP30 overexpressing HELA cells, whereas it was just slightly decreased in control HELA cells, suggesting that ARHGAP30 promoted the degradation of NCL (Figure 5A,B). Furthermore, we found that decreased NCL expression in

ARHGAP30-overexpressing cells could be recovered by adding a proteasome inhibitor MG132 (1  $\mu$ mol/L MG132; Figure 5C). These results indicate that ARHGAP30 might promote NCL degradation via the ubiquitin-proteasomal degradation pathway. Thus, we examined whether ARHGAP30 modulated the ubiquitination of NCL. We overexpressed ubiquitin in both vector control and ARHGAP30 overexpressed HELA cells, followed by western blot to validate overexpression efficiency (Figure 5D). Then we immunoprecipitated NCL and detected its ubiquitination in these cells and found that the ubiquitination of NCL was increased in ARHGAP30 overexpressing cells compared to vector control (Figure 5E). These results demonstrated that ARHGAP30 promoted NCL-ubiquitination mediated degradation to inhibit rRNA synthesis and cell proliferation in cervical cancer cells.

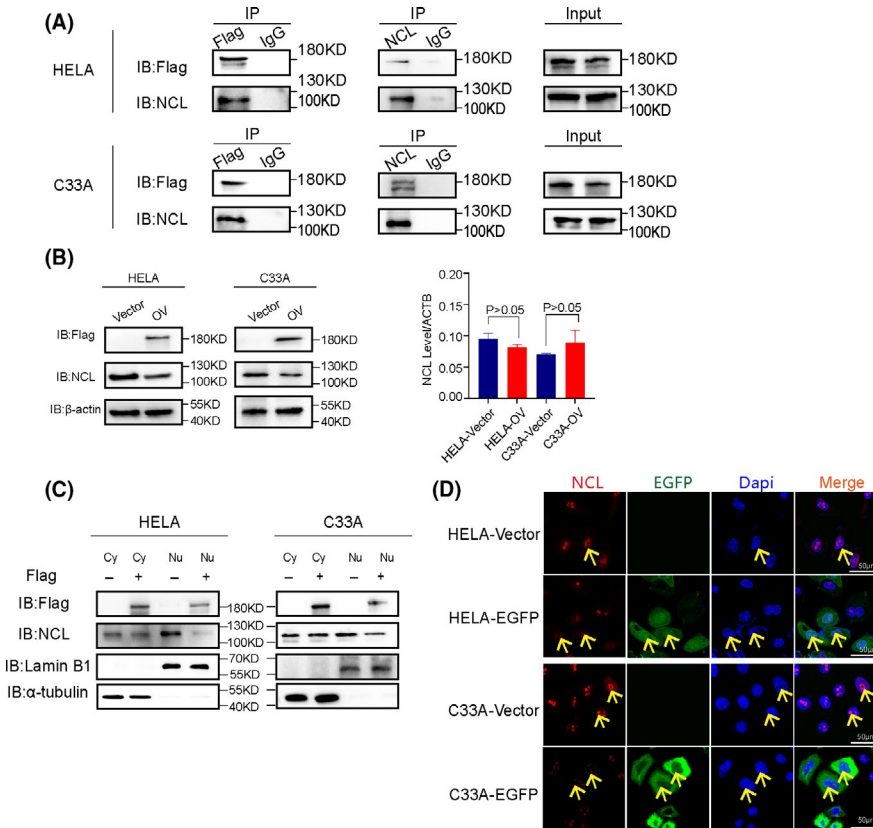


**FIGURE 4** ARHGAP30 interacted with NCL and overexpression of ARHGAP30 reduced NCL expression. A, Co-immunoprecipitation of ARHGAP30-FLAG and NCL in ARHGAP30-FLAG overexpressing HELA and C33A cells. B, Expression of NCL in ARHGAP30-FLAG overexpressing and control cells (left panel). NCL mRNA analysis in ARHGAP30-FLAG overexpressing HELA and C33A and control cells, normalized to ACTB levels (right panel). C, Cytoplasm and nucleus distribution of NCL in ARHGAP30-FLAG overexpress and control cells. Left, Hela cells; right, C33A cells. D, NCL expression decreased in cells overexpressing ARHGAP30-EGFP. Scale bar: 50  $\mu$ m

### 3.7 | Effects of ARHGAP30 on cervical cancer ribosome biogenesis and growth were independent of its RhoGAP activity

Since ARHGAP30 can function independently of RhoGAP activity,<sup>6</sup> we next tested the effects of the RhoGAP-deficient R55A mutant constructs on cervical cancer ribosome biogenesis and growth. We constructed the RhoGAP-deficient plasmid of Flag-tagged ARHGAP30<sup>R55A</sup> using pSLenti-CMV-EGFP-3FLAG vector. This mutant or wild ARHGAP30 expressing plasmid was transfected to low-ARHGAP30 expressing Hela and C33A cells. Then we performed cell growth and cell apoptosis analysis, and we also detected the global protein synthesis. As shown in Figure 6, RhoGAP-deficient ARHGAP30<sup>R55A</sup> had similar suppressive effects on cell proliferation (Figure 6A), global protein synthesis (Figure 6B), and production of pre-rRNA, 5.8S rRNA, and 28S rRNA (Figure 6D) as the wild-type ARHGAP 30. Furthermore, co-immunoprecipitation experiments using an anti-Flag antibody demonstrated that the R55A mutant protein also interacted with NCL in cervical cancer cells (Figure 6C). These results indicate that ARHGAP30 regulates ribosome biogenesis and proliferation independently of its RhoGAP activity in cervical cancer cells.

## 4 | DISCUSSION

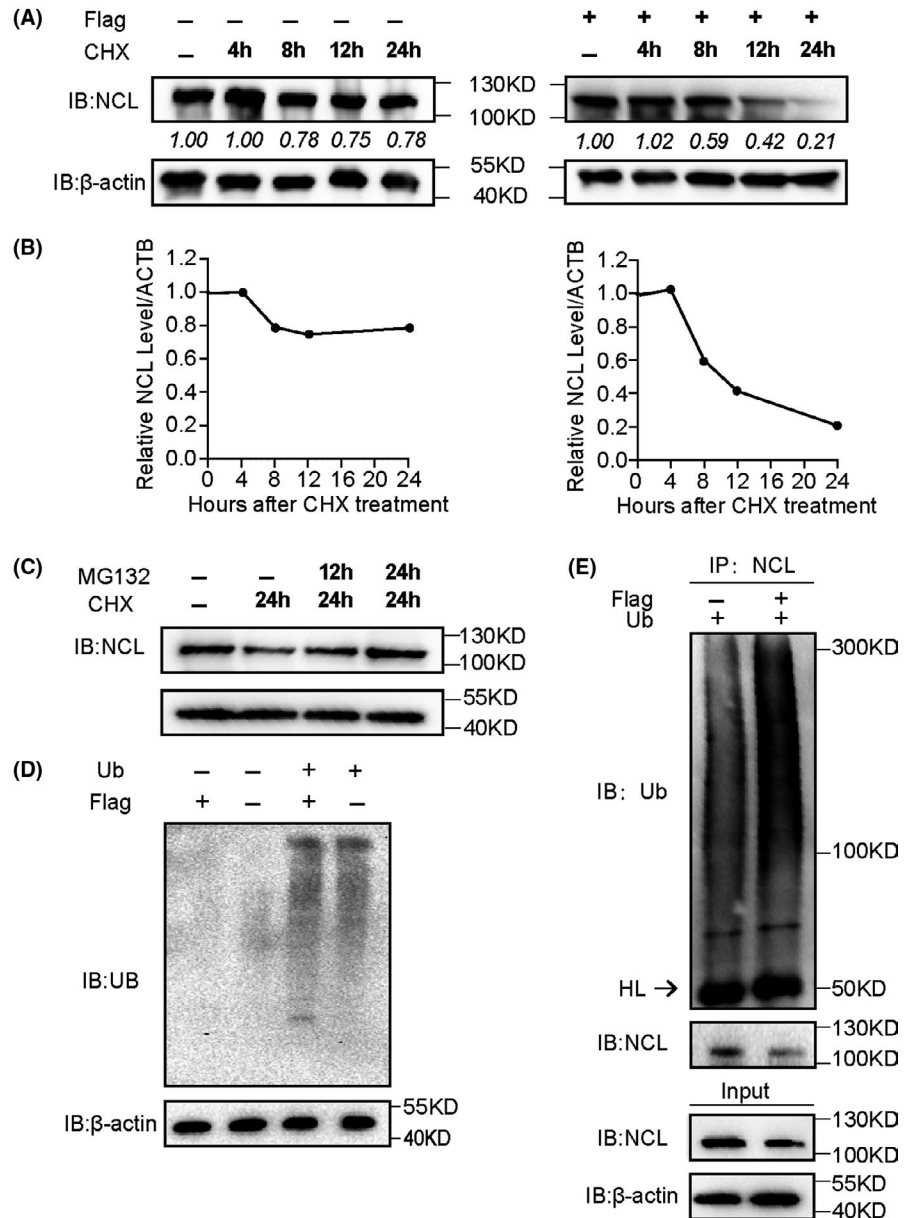
Hyperactivation of ribosome biogenesis initiated by oncogenes or the loss of tumor suppressor genes has critical roles in cancer

initiation and progression.<sup>21</sup> In this study, we found ARHGAP30 is a nucleolus-located protein that was low-expressed in cervical cancers compared to normal cervix tissues and predicted poor prognosis of patients. This finding inspired us to investigate the biological roles and molecular mechanisms of ARHGAP30 in cervical cancer progression. Through a series of functional assays, we uncovered a tumor-suppressing role of ARHGAP30 in cervical cancer both in vitro and in vivo.

Ribosome biogenesis occurred in the nucleolus during the interphase.<sup>22</sup> Ribosomal genes were transcribed by RNA polymerase I to produce the 47S rRNA precursor, which was then processed to generate the mature 18S, 5.8S, and 28S rRNA. The essential role of increased ribosome biogenesis and protein synthesis was to sustain tumor cell growth and proliferation. Our further mechanism investigations revealed a direct link of ARHGAP30 with nucleolar NCL to modulate rRNA transcription and ribosome biogenesis. Ribosome is a complex molecular machine responsible for protein synthesis in living cells. The number of ribosomes was coordinated with the activity of protein synthesis.<sup>23</sup> Our data thus provided a novel functional mechanism of ARHGAP30 in cervical cancer progression that promoted the ubiquitination and degradation of NCL to negatively regulate ribosome-based nascent protein synthesis. ARHGAP30 interacted and colocalized with NCL in the nucleolus and NCL was a major rRNA binding protein of nucleolus associated to pre-ribosomal particles. Previous study found NCL interacted with 40 ribosomal proteins,<sup>10</sup> some of which were also found in ARHGAP30 immunoprecipitates in cervical cancer cells in our study. These ARHGAP30-captured ribosomal proteins may directly interacted



**FIGURE 5** ARHGAP30 promoted the ubiquitination of NCL. A, Western blot of NCL in ARHGAP30-FLAG overexpressing and control cells treated with 25  $\mu\text{g}/\text{mL}$  CHX for 4, 8, 12, and 24 h. B, NCL expression relative to ACTB in A was quantified by image J. Left panel represents the HeLa-Vector group and right panel represents the HeLa-OV group. C, Western blot of NCL in HeLa-OV cells treated with 25  $\mu\text{g}/\text{mL}$  CHX alone or co-treated with MG132 for the indicated time. D, HeLa-Vector and HeLa-OV cells were transfected with pCMV-V5-Ub plasmid and harvested for western blot analysis of its expression. E, Ubiquitination was detected using an anti-UB antibody. HeLa-Vector and HeLa-OV cells were transfected with pCMV-V5-Ub. After 36 h, the cells were treated with MG132 for 12 h, then lysates were immunoprecipitated with a NCL antibody and detected by western blot



with ARHGAP30 or indirectly through interaction with NCL. The details and biological functions of these possible interactions are worthy of further investigations.

NCL was involved in the tumorigenesis by increasing rRNA synthesis and ribosome assembly.<sup>24</sup> We found ARHGAP30 interacted with NCL and promoted ubiquitination of NCL. ARHGAP30 also reduced the level of pre-rRNA, 28S, and 5.8S in cervical cancer cells, but how ARHGAP30 regulates the ubiquitination of NCL remains unresolved. A previous study found NCL ubiquitination was regulated by CSA, a component of E3 ligase complex.<sup>25</sup> p250GAP, another member of RhoGAPs, was reported as a novel interactor of the E3 ubiquitin ligase Cdh1-APC.<sup>26</sup> These clues suggest that ARHGAP30 may possibly be involved in the NCL/E3 ligase complex machine.

Studies have reported that ribosomal biogenesis stress will activate p53<sup>27</sup> and NCL has been suggested to be associated with p53. In our study, we found the function of ARHGAP30 on ribosome

biogenesis was similar in different cervical cancer cell lines with different p53 status (low p53 in HeLa and mutant p53 in C33A). The expression levels of p53 and acetylated p53 were not obviously affected by ARHGAP30 overexpression in these cells (Figure S2B). The transcription levels of p53 target genes PUMA, P21 and BAX were not affected either (Figure S2B). Therefore, ARHGAP30 might regulate NCL stability independently of p53 in cervical cancer cells.

Rho GTPases are well-known regulators of the actin cytoskeleton, which contribute to cell migration.<sup>28</sup> ARHGAP30 is also involved in actin dynamics.<sup>5</sup> In this study, we found ARHGAP30 inhibited the migration and promoted the apoptosis of cervical cancer cells. Analysis of ARHGAP30 immunoprecipitated proteins resulted in focal adhesion enriched gene sets (Table S1). One of these is TRIP6, which is localized in focal adhesion plaques and associated with the actin cytoskeleton.<sup>29</sup> A number of studies have verified that TRIP6 acts as a mediator of cancer migration and invasion.<sup>30</sup>

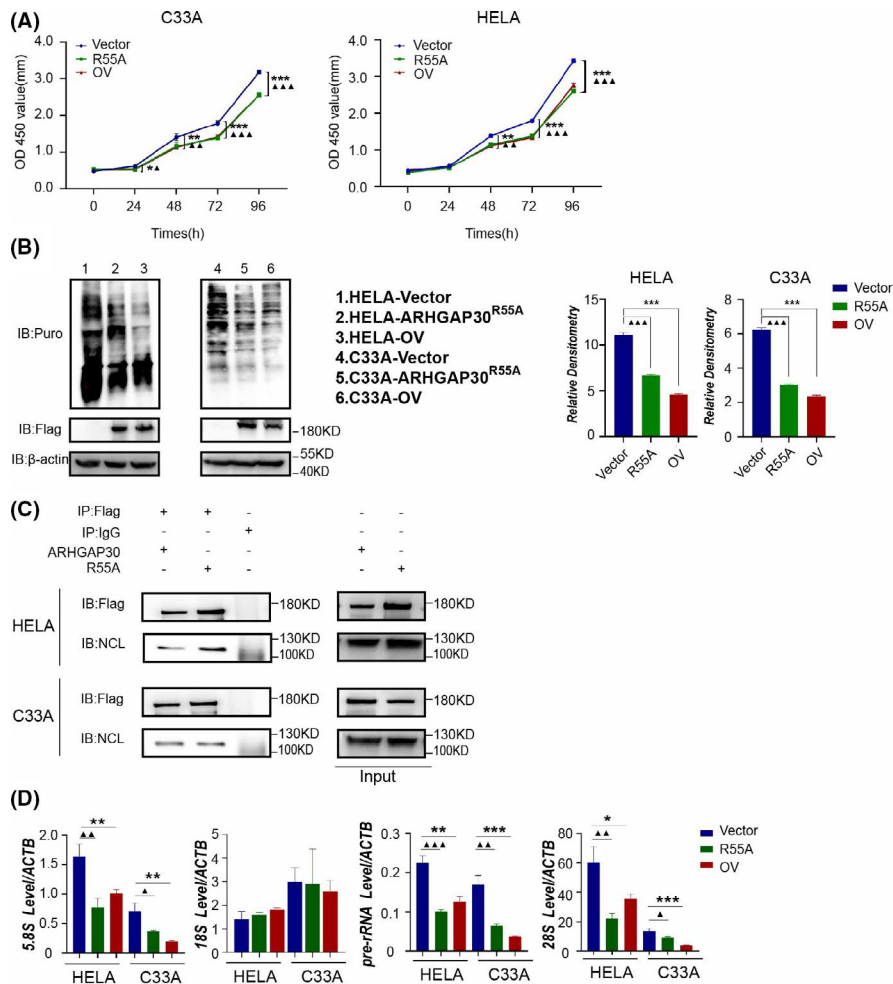


**FIGURE 6** ARHGAP30 can function RhoGAP-independently. **A**, Analysis of cervical cancer cell proliferation in vitro. Results are shown as the means  $\pm$  standard deviation of the OD 450 value. **B**, Western blot of puromycin-labeled nascent proteins. Puromycin (10  $\mu$ mo/L) was added to the medium of HELA and C33A cells 20 min before harvest. Anti-Flag antibody was used to detect the exogenous expression of ARHGAP30 (R55A) and ARHGAP30.  $\beta$ -actin (ACTB) was detected as an internal control. Relative quantification of the density of western blot bands was shown on the right panel. **C**, Co-immunoprecipitation of FLAG and NCL in ARHGAP30<sup>R55A</sup> and ARHGAP30 overexpressing HELA and C33A cells. **D**, Analysis of pre-rRNA, 28S, 5.8S, and 18S rRNA level in control HELA, C33A cells and ARHGAP30<sup>R55A</sup>, ARHGAP30 overexpression cells, normalized to ACTB. Vector vs R55A: \*P < .05; \*\*P < .01; \*\*\*P < .001. Vector vs ARHGAP30: \*P < .05; \*\*P < .01; \*\*\*P < .001

In cervical cancer, TRIP6 is upregulated and contributes to Yes-associated protein (YAP) activation by downregulating the level of YAP phosphorylation.<sup>31</sup> TRIP6 participates in cell migration by controlling reorganization of the actin cytoskeleton at the contact sites through downregulating Rac1 and possibly by upregulating RhoA activity.<sup>32</sup> ARHGAP30 regulated F-actin dynamic and Rac1, RhoA activity. F-actin accumulation would inactivate YAP phosphorylation.<sup>33,34</sup> ARHGAP30 overexpression might therefore suppress cervical cancer cell migration by coordination with TRIP6 and F-actin/Hippo-YAP signaling, which is worthy of future investigation.

#### ACKNOWLEDGMENTS

This research was supported by the Natural Science Foundation of Shanghai (grant no. 17ZR1421400 to Dr Zhihong Ai). We thank Shanghai Bioprofile Technology Company Ltd for technical support in mass spectrometry.

#### DISCLOSURE

The authors have no conflict of interest.

#### ORCID

Lan Lin <https://orcid.org/0000-0003-4778-0887>

Zhihong Ai <https://orcid.org/0000-0002-8220-8192>

#### REFERENCES

- Bray F, Ferlay J, Soerjomataram I, et al. Global cancer statistics 2018: GLOBOCAN estimates of incidence and mortality worldwide for 36 cancers in 185 countries. *CA: Cancer J Clin*. 2018;68(6):394-424.
- Kumar L, Harish P, Malik PS, Khurana S. Chemotherapy and targeted therapy in the management of cervical cancer. *Curr Probl Cancer*. 2018;42(2):120-128.
- Pan Q, Xu J, Ma L. Simvastatin enhances chemotherapy in cervical cancer via inhibition of multiple prenylation-dependent GTPases-regulated pathways. *Fundam Clin Pharmacol*. 2020;34(1):32-40.
- Liu X, Chen D, Liu G. Overexpression of RhoA promotes the proliferation and migration of cervical cancer cells. *Biosci Biotechnol Biochem*. 2014;78(11):1895-1901.
- Naji L, Pacholsky D, Aspenstrom P. ARHGAP30 is a Wrch-1-interacting protein involved in actin dynamics and cell adhesion. *Biochem Biophys Res Commun*. 2011;409(1):96-102.
- Wang J, Qian J, Hu Y, et al. ArhGAP30 promotes p53 acetylation and function in colorectal cancer. *Nat Commun*. 2014;5(4735):1-15.
- Zhou Y, Hua Z, Zhu Y, et al. Upregulation of ARHGAP30 attenuates pancreatic cancer progression by inactivating the beta-catenin pathway. *Cancer Cell Int*. 2020;20:225.
- Mao X, Tong J. ARHGAP30 suppressed lung cancer cell proliferation, migration, and invasion through inhibition of the Wnt/beta-catenin signaling pathway. *Oncotargets Ther*. 2018;11:7447-7457.
- Catez F, Dalla Venezia N, Marcel V, et al. Ribosome biogenesis: an emerging druggable pathway for cancer therapeutics. *Biochem Pharmacol*. 2019;159:74-81.

10. Yanagida M, Shimamoto A, Nishikawa K, et al. Isolation and proteomic characterization of the major proteins of the nucleolin-binding ribonucleoprotein complexes. *Proteomics*. 2001;1:1390-1404.
11. Salvetti A, Coute Y, Epstein A, et al. Nuclear functions of nucleolin through global proteomics and interactomic approaches. *J Proteome Res*. 2016;15(5):1659-1669.
12. Grinstein E, Wernet P, Snijders PJ, et al. Nucleolin as activator of human papillomavirus type 18 oncogene transcription in cervical cancer. *J Exp Med*. 2002;196:1067-1078.
13. Meng GZ, Zi Y, Li HQ, Huang M, Gao T. Nucleolin expression is correlated with carcinogenesis and progression of cervical squamous cell carcinoma. *Nan Fang Yi Ke Da Xue Xue Bao*. 2015;35(10):1511-1514.
14. Liu F, Dai M, Xu Q, et al. SRSF10-mediated IL1RAP alternative splicing regulates cervical cancer oncogenesis via mLL1RAP-NF-kappaB-CD47 axis. *Oncogene*. 2018;37:2394-2409.
15. Kelleher AR, Kimball SR, Dennis MD, Leonard SJ. The mTORC1 signaling repressors REDD1/2 are rapidly induced and activation of p70S6K1 by leucine is defective in skeletal muscle of an immobilized rat hindlimb. *Am J Physiol Endocrinol Metab*. 2013;304(2):E229-E236.
16. Kainulainen M, Lau S, Samuel CE, Hornung V, Webera F. NSs virulence factor of rift valley fever virus engages the F-box proteins FBXW11 and beta-TRCP1 to degrade the antiviral protein kinase PKR. *J Virol*. 2016;90(13):6140-6147.
17. Caudron-Herger M, Pankert T, Rippe K. Regulation of nucleolus assembly by non-coding RNA polymerase II transcripts. *Nucleus*. 2016;7(3):308-318.
18. Stepinski D. The nucleolus, an ally, and an enemy of cancer cells. *Histochem Cell Biol*. 2018;150(6):607-629.
19. Ko CY, Lin CH, Chuang JY, Chang WC, Hsu TI. MDM2 degrades deacetylated nucleolin through ubiquitination to promote glioma stem-like cell enrichment for chemotherapeutic resistance. *Mol Neurobiol*. 2018;55(4):3211-3223.
20. Chen Z, Xu X. Roles of nucleolin. Focus on cancer and anti-cancer therapy. *Saudi Med J*. 2016;37(12):1312-1318.
21. Orsolic I, Jurada D, Pullen N, et al. The relationship between the nucleolus and cancer: current evidence and emerging paradigms. *Semin Cancer Biol*. 2016;37-38:36-50.
22. McLeod T, Abdullahi A, Li M, Brogna S. Recent studies implicate the nucleolus as the major site of nuclear translation. *Biochem Soc Trans*. 2014;42(4):1224-1228.
23. Derenzini M, Montanaro L, Trere D. Ribosome biogenesis and cancer. *Acta Histochem*. 2017;119(3):190-197.
24. Jia W, Yao Z, Zhao J, Guan Q, Gao L. New perspectives of physiological and pathological functions of nucleolin (NCL). *Life Sci*. 2017;186:1-10.
25. Bohr VA, Croteau DL, Demarest TG, et al. Cockayne syndrome group A and B proteins function in rRNA transcription through nucleolin regulation. *Nucleic Acids Res*. 2020;48(5):2473-2485.
26. Kannan M, Lee SJ, Schwedhelm-Domeyer N, Nakazawa T, Stegmuller J. p250GAP is a novel player in the Cdh1-APC/Smurf1 pathway of axon growth regulation. *PLoS One*. 2012;7(11):e50735.
27. Golomb L, Volarevic S, Oren M. p53 and ribosome biogenesis stress: the essentials. *FEBS Lett*. 2014;588(16):2571-2579.
28. Croise P, Estay-Ahumada C, Gasman S, Stéphane O. Rho GTPases, phosphoinositides, and actin: a tripartite framework for efficient vesicular trafficking. *Small GTPases*. 2014;5:e29469.
29. Lin VT, Lin FT. TRIP6: an adaptor protein that regulates cell motility, antiapoptotic signaling and transcriptional activity. *Cell Signal*. 2011;23(11):1691-1697.
30. Willier S, Butt E, Richter GH, Burdach S, Grunewald TG. Defining the role of TRIP6 in cell physiology and cancer. *Biol Cell*. 2011;103(12):573-591.
31. Yang F, Li L, Zhang J, Zhang J, Yang L. TRIP6 accelerates the proliferation and invasion of cervical cancer by upregulating oncogenic YAP signaling. *Exp Cell Res*. 2020;396(1):112248.
32. Bai CY, Ohsugi M, Abe Y, Tadashi Y. ZRP-1 controls Rho GTPase-mediated actin reorganization by localizing at cell-matrix and cell-cell adhesions. *J Cell Sci*. 2007;120(Pt 16):2828-2837.
33. Zhang YL, Li Q, Yang XM, et al. SPON2 promotes M1-like macrophage recruitment and inhibits hepatocellular carcinoma metastasis by distinct integrin-Rho GTPase-hippo pathways. *Cancer Res*. 2018;78(9):2305-2317.
34. Yang XM, Cao XY, He P, et al. Overexpression of Rac GTPase activating protein 1 contributes to proliferation of cancer cells by reducing hippo signaling to promote cytokinesis. *Gastroenterology*. 2018;155(4):1233-1249.e22.

## SUPPORTING INFORMATION

Additional supporting information may be found in the online version of the article at the publisher's website.

**How to cite this article:** Wu A, Lin L, Li X, et al.

Overexpression of ARHGAP30 suppresses growth of cervical cancer cells by downregulating ribosome biogenesis. *Cancer Sci*. 2021;112:4515-4525. <https://doi.org/10.1111/cas.15130>